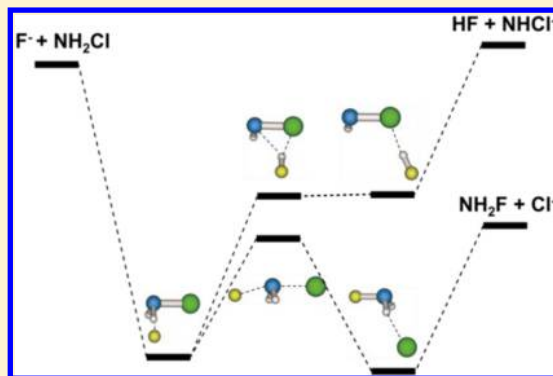


Theoretical Studies on $F^- + NH_2Cl$ Reaction: Nucleophilic Substitution at Neutral Nitrogen

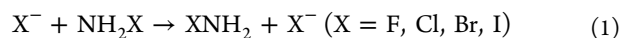
Xu Liu,[†] Jiaxu Zhang,^{*,†} Li Yang,^{*,†} and Rui Sun[‡][†]School of Chemistry and Chemical Engineering Harbin Institute of Technology Harbin 150001, P. R. China[‡]Department of Chemistry University of Chicago Chicago, Illinois 60637, United States**S** Supporting Information

ABSTRACT: The S_N2 reactions at N center, denoted as $S_N2@N$, has been recognized to play a significant role in carcinogenesis, although they are less studied and less understood. The potential energy profile for the model reaction of $S_N2@N$, chloramine (NH_2Cl) with fluorine anion (F^-), has been characterized by extensive electronic structure calculations. The back-side S_N2 channel dominates the reaction with the front-side S_N2 channel becoming feasible at higher energies. The minimum energy pathway shows a resemblance to the well-known double-well potential model for S_N2 reactions at carbon. However, the complexes involving nitrogen on both sides of the reaction barrier are characterized by $NH\cdots X$ ($X = F$ or Cl) hydrogen bond and possess C_1 symmetry, in contrast to the more symmetric ion-dipole carbon analogues. In the $F^- + NH_2Cl$ system, the proton transfer pathway is found to become more competitive with the S_N2 pathway than in the $F^- + CH_3Cl$ system. The calculations reported here indicate that stationary point properties on the $F^- + NH_2Cl$ potential energy surface are slightly perturbed by the theories employed. The MP2 and CAM-B3LYP, as well as M06-2X and MPW1K functionals give overall best agreement with the benchmark CCSD(T)/CBS energies for the major S_N2 reaction channel, and are recommended as the preferred methods for the direct dynamics simulations to uncover the dynamic behaviors of the title reaction.



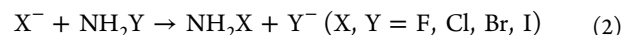
I. INTRODUCTION

Bimolecular nucleophilic substitution (S_N2) reactions are known for their rich reaction dynamics and are of fundamental importance in chemistry.^{1–8} Compared to the well characterized S_N2 process at carbon (C), displacement at nitrogen (N) remains less understood. The S_N2 reactions at N center play significant roles in both organic synthesis and carcinogenesis,^{9,10} and therefore, have been attracting an increasing amount of attention.^{11–16} By means of double labeling experiments, the existence of a classical S_N2 transition state (TS) at a nitrogen substrate has been inferred in experiment.¹⁷ From a theoretical point of view, the topology of the potential energy surface (PES) for $S_N2@N$ in gas phase is characterized by double-well energy profile, with two minima corresponding to the formation of hydrogen-bonded complex and with a transition structure of C_{2v} symmetry (see Figure 1).^{18–22} High-level G2(+) calculations for identity S_N2 reactions 1 predict that the overall barrier, i.e., the S_N2 TS energies relative to reactants, are negative for all halogens, in contrast to the analogous reactions at carbon where the barrier is negative only for fluorine.²³



These studies indicate that nucleophilic displacement may be more facile at nitrogen than at carbon. Hybrid density function

theory (DFT) methods have been assessed in describing identity S_N2 reactions^{1,22} and the DFT calculations have been used to analyze the nonidentity S_N2 reactions^{2,4}



The slightly higher central barriers, i.e., the S_N2 TS energies relative to reactant complex, for reactions with NH_2Y than for the corresponding reactions with CH_3Y are revealed. Moreover, the overall barriers for reactions 2 are found to be lower than those of carbon reactions, in line with the prediction for identity S_N2 reactions 1. Recently, Yu carried out a detailed evaluation of the performance of MP2 and many DFT functionals for describing PESs of a wide range of nitrogen S_N2 reactions.²⁵ The dynamical information is more limited for the displacement at N. Ab initio trajectory calculations have been applied to study the $F^- + NH_2F$ and $OH^- + NH_2Y$ ($Y = F$ and Cl) systems and the important nonstatistical behaviors have been suggested.²⁶

The $F^- + CH_3Y \rightarrow CH_3F + Y^-$ ($Y = Cl$ and I) reactions are of particular interest since their PESs are substantially different than the conventional double-well model that characterizes gas

Received: April 5, 2016

Revised: May 4, 2016

Published: May 4, 2016



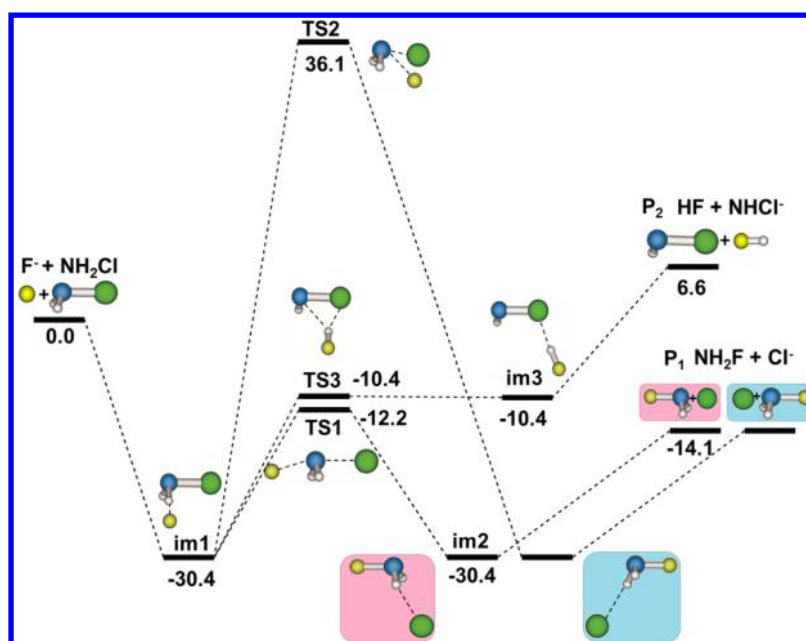


Figure 1. Potential energy curves and stationary points for the CCSD(T)/CBS PES for the $F^- + NH_2Cl$ reaction. The back-side attack and front-side attack S_N2 pathways lead to inversion (pink) and retention (blue) of the initial configuration. The potential energies in kcal/mol are classical energies without zero point energy (ZPE).

phase S_N2 reactions at C center.^{2,5,27,28} A hydrogen-bonded complex of C_s symmetry ($F^- \cdots HCH_2Y$) is found as a minimum energy structure in the entrance channel for both reactions together with a second close lying ion-dipole complex of colinear C_{3v} symmetry ($F^- \cdots CH_3Y$). Despite their similar PES structures, the dynamics show qualitatively different features.²⁸ In contrast to the dominant direct rebound mechanism identified for the $F^- + CH_3Cl$ reaction, an indirect mechanism with formation of the $F^- \cdots HCH_2I$ hydrogen-bonded complex is found to play an important part in the $F^- + CH_3I$ dynamics. A hydrogen-bonded $F^- \cdots NH_2Cl$ entrance channel structure has been predicted for the nitrogen S_N2 reaction $F^- + NH_2Cl$.¹⁹ An interesting issue is whether the reaction dynamics of NH_2Cl are similar to those of CH_3Cl or CH_3I .

Using the tandem flowing afterglow-selected ion flow tube (FA-SIFT) technique,²⁹ Bierbaum et al. have investigated the reaction kinetics of NH_2Cl with F^- at room temperature and found that this reaction is approximately two times faster than the analogous S_N2 reaction of CH_3Cl . The measured product branching ratio indicates that nucleophilic substitution at nitrogen to form Cl^- is the dominant reaction pathway with no proton abstraction to yield $NHCl^-$ observed, and the detailed atomic-level reaction mechanisms are needed to understand this observation.

Interpreting the dynamics and kinetics of S_N2 reactions and comparing with experiments, by either statistical calculations or chemical dynamics simulations, requires accurate PESs. In the work presented here, stationary point properties of $F^- + NH_2Cl$ reaction are calculated by using the DFT with different functionals, MP2, and CCSD(T) theories. To determine the preferred method for a direct dynamics simulation, comparisons are made between the results of these calculations and with experimental and previously obtained theoretical results. The similarities and differences between the reaction of NH_2Cl with F^- and the corresponding reaction of CH_3Cl are revealed. This work may provide an insight into the S_N2 mechanism at nitrogen center.

II. COMPUTATIONAL METHODS

The stationary point properties for the reactants, products, intermediates, and transition states on the $F^- + NH_2Cl$ PES are determined using the MP2^{30,31} and DFT,^{32–35} with the M06-2X, CAM-B3LYP, B97-1, B3LYP, M06, and MPWIK functionals, which are selected from ref 25. The correlation-consistent double- ζ basis set of Dunning augmented with diffuse functions, aug-cc-pVDZ (abbreviated to DZ),^{36,37} is employed for the calculations. The stationary nature of the structures is confirmed by harmonic vibrational frequency calculations, that is, the potential minima possess all real frequencies, whereas the transition state possesses only one imaginary frequency. The harmonic zero-point energy (ZPE) is obtained at all the above levels of theory. To ensure that the transition states connect designated minima, the intrinsic reaction coordinate (IRC)³⁸ is calculated for both directions off the saddle point at both the MP2/DZ and DFT/DZ levels of theory. To obtain more reliable energies, higher level single-point energy calculations were performed at the CCSD(T) level of theory.³⁹ The calculations were performed with the correlation consistent Gaussian basis sets, denoted by aug-cc-pVXZ, where X is the cardinal number for the basis set (X = D, T, Q, and 5).^{36,37} For simplicity, aug-cc-pVXZ is abbreviated to XZ. The results were extrapolated to the complete basis set (CBS) limit using the formula proposed by Peterson et al.⁴⁰

$$E(n) = E_{\text{CBS}} + A \exp[-(n-1)] + B \exp[-(n-1)^2] \quad (3)$$

where $n = 2, 3, 4$, and 5 , representing the DZ, TZ, QZ, and 5Z basis sets, respectively. The CCSD(T) calculations are based on MP2/DZ minimum geometries. Unless otherwise specified, the CCSD(T)/CBS energies are used in the following discussions. The NWChem system of programs⁴¹ was used to perform most of the above electronic structure calculations. Gaussian09⁴² was used to calculate the IRCs.

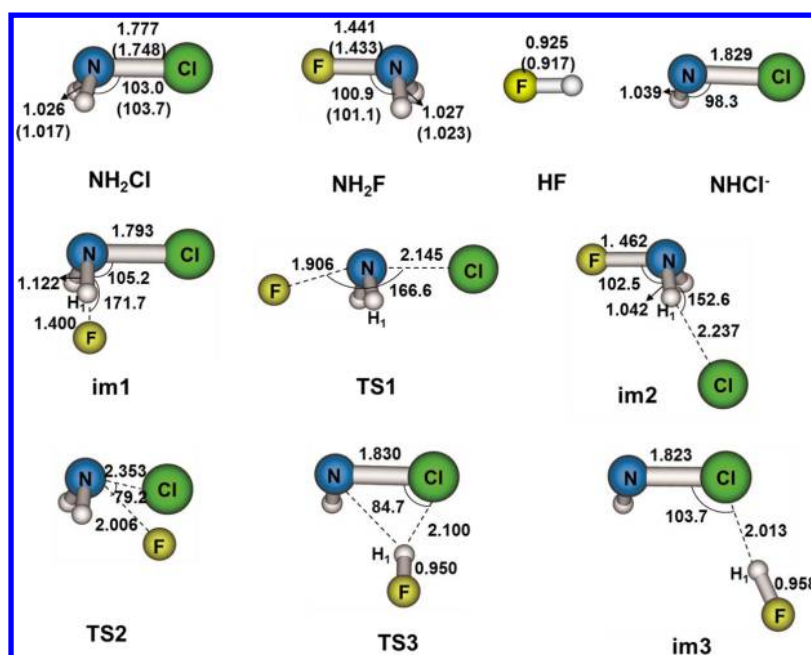


Figure 2. Geometries of stationary points for the $F^- + NH_2Cl$ reaction optimized at the MP2/DZ level of theory. Bond distances are in Å and angles in degrees. The available experimental values (refs 43–45) are in parentheses.

III. RESULTS AND DISCUSSION

A. Potential Energy Surface. Figure 1 presents the potential energy curve and relative energies of stationary points for the CCSD(T)/CBS PES. Initially, the reactants come together to form a hydrogen-bonded $F^- \cdots NH_2Cl$ (**im1**) pre-reaction complex, starting from which, both S_N2 and proton transfer (PT) reaction pathways are open for the $F^- + NH_2Cl$ reaction. The S_N2 pathways at nitrogen may take place by either front- or back-side attack. The back-side attack of F^- on NH_2Cl proceeds via **TS1** and forms the hydrogen-bonded $FNH_2 \cdots Cl^-$ (**im2**) post-reaction complex, followed by its dissociation giving products P_1 $NH_2F + Cl^-$ with the inversion of the initial configuration. For the minimum energy pathway involving front-side nucleophilic attack at nitrogen, complex **im1** must overcome a higher activation barrier to reach transition structure **TS2**. The energy then drops with the formation of complex **im2** which finally dissociates into separated S_N2 products P_1 with the retention of configuration.

The optimized structures of stationary points as well as the available experimental values are predicted in Figure 2. The geometries of the pre- and post-reaction complexes **im1** and **im2** determined by MP2 and DFT show that the halogen atom is bonded to one hydrogen atom, and it can switch between two H atoms with a barrier of 6.9 kcal/mol or less. Notably, the IRC calculations with M06-2X/DZ found that S_N2 transition states **TS1** and **TS2** connect a post-reaction complex **im2'** instead of **im2**, with inversion or retention of the initial NH_2 configuration, for which Cl^- is bonded to both H atoms. Complex **im2'** can easily interconvert with **im2** via a transition state **TS22'**. The calculated M06-2X PES together with the structures of **im2'** and **TS22'** are illustrated in Figures S1 and S2 in the Supporting Information. However, these two structures are not found with other theories, despite numerous attempts. This may be not unexpected, given that the PES is very flat in the vicinity of complexes **im2** and **im2'** and transition state **TS22'**, which are almost isoenergetic (-36.7 kcal/mol) at the M06-2X/DZ level of theory (see Figures S1).

The MP2 and DFT calculations with different functionals for the proton transfer pathway predict the existence of the pre-reaction complex **im1** and a transition state **TS3** connecting this complex with a post-reaction complex $NHCl^- \cdots HF$ (**im3**). In this reaction path, **im1** undergoes a concerted H-shift from the N to F atom and a migration of HF from the N to Cl atom forming **im3**, which undergoes hydrogen bond rupture resulting in products P_2 $HF + NHCl^-$. It is noted that the structures **TS3** and **im3** are very similar in energy with the latter is only 0.3–1.1 kcal/mol lower with respect to the former at the MP2 and DFT theories with ECP/d basis set. The higher level CCSD(T) calculations give the isoenergetic CBS values for these two structures (Figure 1). Thus, the PES in the vicinity of transition state **TS3** and complex **im3** is rather flat.

Our CCSD(T)/CBS calculations presented in Figure 1 allow an assessment of the likelihood of the proton transfer pathway in comparison with the two S_N2 pathways. In going from pre-reaction complex **im1** to products, the barriers are 18.2, 66.5, and 37.0 kcal/mol for the back-side inversion S_N2 (**im1** \rightarrow **TS1**), front-side retention S_N2 (**im1** \rightarrow **TS2**), and proton transfer (**im1** \rightarrow P_2) reactions, respectively. Given that the barrier for front-side S_N2 pathway is substantially greater than that for proton transfer pathway, the latter is generally preferred over the former. However, the proton transfer pathway is much less competitive than the back-side S_N2 pathway in view of the considerably smaller barrier for the latter. As a result, the back-side inversion S_N2 is kinetically the most feasible pathway for the $F^- + NH_2Cl$ reaction.

Since transition state **TS2** (36.1 kcal/mol) lies much higher than reactants $F^- + NH_2Cl$, the front-side retention pathway is expected to only contribute to the S_N2 reaction at higher energies. The energies for the back-side S_N2 and proton transfer pathways are submerged with respect to the energy of reactants, except for the products P_2 $HF + NHCl^-$, which lies 6.6 kcal/mol above the reactants. Thus, these two pathways may well be followed at relatively low energies. In view of the

threshold energy for proton transfer, our calculations predict this reaction channel may not be observed at the room temperature, in line with the estimated branching ratio of 1.0/0.0 for S_{N2} /proton transfer in the experiments at 300 K.²⁹

B. Properties of the Stationary Points. To test the influence of methodology on the $F^- + NH_2Cl$ PES, MP2, and six different DFT functionals with ECP/d basis set are employed to investigate the stationary point properties, and the comparison between these calculations are presented in the following.

Geometries. The stationary point geometries are listed in Table S1 in the Supporting Information and depicted in Figure 2. Overall, the MP2 and DFT structures for the S_{N2} and proton transfer pathways are similar. Variations in bond lengths are generally less than ~ 0.1 Å and the largest difference lies in nitrogen-halogen bond lengths of TS2. The MP2 bond angles agree well with the DFT values in most cases with difference of $\sim 3^\circ$ or less. The geometries of NH_2Cl reactant, NH_2F S_{N2} product, and HF PT product obtained at the different levels of theory are compared with experiment^{43–45} in Table S1. The calculated bond lengths and bond angles are not sensitive to the theoretical methods. CAM-B3LYP gives the best agreement with experiment. In addition, the determined geometries of NH_2Cl , NH_2F , and the stationary point structures for the back-side S_{N2} pathway are in general consistent with those obtained previously by MP2/6-31+G(d)⁴⁶ and MPW1K/6-31+G(d,p) theories¹⁴ as shown in Table S1.

Vibrational Frequencies. Vibrational Frequencies are listed in Table S2 of the Supporting Information. In general, the MP2 and DFT frequencies are in agreement with the relative discrepancy less than 5% for most of the vibrational modes. The large difference mainly lies in TS2, for which DFT frequencies are consistent for each functionals, but overall substantially smaller than MP2 values with discrepancy around 20%. Good agreement between DFT/M06-2X and MP2 is found for the imaginary reaction coordinate frequencies of transition states TS1–TS3. However, MP2 imaginary frequencies of TS1 and TS2 for S_{N2} substitution are substantially larger than other DFT values. The higher imaginary frequencies of the TS1 and TS2 with MP2 theory correspond to a “steeper” saddle point on the energy hypersurface and can be associated with a relatively tight transition state structure (see Table S1). In contrast, for the PT pathway MP2 gives the imaginary frequency of TS3 lower than those of DFT functionals. These results indicate that the MP2 and DFT theories give the different potential energy surface shapes in the vicinity of the dynamical bottleneck for the S_{N2} and proton transfer reactions. In addition, the calculated frequencies of the NH_2Cl reactant and NH_2F and HF products are in good agreement with experiment,^{47–49} and DFT B3LYP and B97-1 functionals give the best agreement with an average deviation of 3%.

Energies. Benchmark calculations are carried out with CCSD(T) method, extrapolated to the complete basis set limit as described in Section II. The resulting energies and the CBS values are listed in Table 1. The CCSD(T)/CBS energies for the stationary points are 0–0.5 kcal/mol different from the CCSD(T)/SZ values, which shows good convergence toward the complete basis set limit for the CCSD(T) energies. Table 2 displays the relative energies for the stationary points calculated with MP2 and DFT functionals using the ECP/d basis set, as well as the CCSD(T)/CBS energies. The MP2 energies are overall higher in comparison with DFT values and different theories give quite a range of energies for each stationary point.

Table 1. CCSD(T) Energies for $F^- + NH_2Cl$ Stationary Points^{a,b}

stationary point	basis set				
	DZ	TZ	QZ	SZ	CBS
im1 $F^- \cdots NH_2Cl$	−30.2	−30.6	−30.6	−30.4	−30.4
TS1	−16.2	−13.6	−13.2	−12.7	−12.2
im2 $FNH_2 \cdots Cl^-$	−32.0	−30.9	−30.9	−30.5	−30.4
P ₁ $Cl^- + NH_2F$	−15.7	−14.3	−14.5	−14.1	−14.1
TS2	31.2	34.3	35.1	35.7	36.1
TS3	−7.8	−10.0	−10.2	−10.2	−10.4
im3 $HF \cdots NHCl^-$	−8.0	−10.4	−10.6	−10.7	−10.4
P ₂ $HF + NHCl^-$	9.2	7.4	6.9	6.8	6.6

^aEnergies (kcal/mol) are with respect to the reactants $F^- + NH_2Cl$ and do not include zero-point energy (ZPE). ^bThe aug-cc-pVXZ basis sets, abbreviated to XZ, X = D, T, Q, and S, are used for CCSD(T) calculations. The CCSD(T) calculations are based on MP2/DZ minimum geometries.

The energies found with the MP2 and various DFT levels of theory, are compared with the benchmark energies to evaluate the accuracy of different theories. For the dominant back-side S_{N2} pathway, the MP2 and CAM-B3LYP theories give the better accuracy than do the other DFT functionals. The reaction barriers play an important role in the S_{N2} kinetics and dynamics. In this respect, M06-2X and MPW1K present good performance besides MP2 and CAM-B3LYP. The CCSD(T)/CBS values for the central barrier (im1 \rightarrow TS1) and overall barrier (reactants \rightarrow TS1) of back-side S_{N2} reaction are 18.2 and −12.2 kcal/mol, which are close to the MP2 (18.8 and −10.8 kcal/mol), CAM-B3LYP (15.2 and −15.8 kcal/mol), M06-2X (19.0 and −14.1 kcal/mol), and MPW1K (17.0 and −14.3 kcal/mol) values, but much higher than those of other functionals, as shown in Table 2. On the other hand, MPW1K and M06-2X have somewhat higher systematic errors due to the lower energies of im2 and P₁ compared with the benchmark. B3LYP reproduces the features of all the stationary points, with the exception of underestimation of the overall barrier height by ~ 7.8 kcal/mol.

For the proton transfer pathway, M06-2X, B97-1, M06, and MPW1K give the precision within 2.2 kcal/mol, while other theories, especially MP2, result in relatively larger energy difference from CCSD(T)/CBS with a maximum deviation of 2.2–5.1 kcal/mol. For the high energy TS2 of front-side S_{N2} attack, the M06-2X and MPW1K agrees very well with the CCSD(T)/CBS energy, with a small difference within 0.6 kcal/mol, but the substantial variations (4.3–12.2 kcal/mol) from CCSD(T)/CBS value are still found for other theories, indicating the high energy regions of the PESs given by these theories in the vicinity of TS2 might be less accurate.

As seen in Figure 1, energetically, the most favored one among different reaction channels for the $F^- + NH_2Cl$ system is the back-side S_{N2} pathway, which is more competitive than the proton transfer pathway at lower energies. Taking this into consideration, MP2 and CAM-B3LYP, as well as M06-2X and MPW1K may be chosen as the most practical methods to perform the direct dynamics calculations of the $F^- + NH_2Cl$ reaction to understand the experimental results obtained by Bierbaum et al.,²⁹ which were carried out at 300 K, corresponding to a collision energy of ~ 0.04 eV.

C. Comparison with $F^- + CH_3Cl$ Reaction. It is of interest to compare PES features of the title $F^- + NH_2Cl$ reaction with that of the analogous reaction $F^- + CH_3Cl$, which has been

Table 2. Electronic Structure Theory Energies for $F^- + NH_2Cl$ Stationary Points.^{a,b}

stationary points	theory							
	MP2	M06-2X	CAM-B3LYP	B97-1	B3LYP	M06	MPW1K	CCSD(T)/CBS
im1 $F^- \cdots NH_2Cl$	-29.6	-33.1	-31.0	-31.5	-30.5	-31.1	-31.3	-30.4
TS1	-10.8	-14.1	-15.8	-20.2	-20	-20.1	-14.3	-12.2
im2 $FNH_2 \cdots Cl^-$	-29.2	-36.7	-33.8	-34	-32.8	-34.0	-35.4	-30.4
P₁ $NH_2F + Cl^-$	-13.0	-20.4	-17.5	-17.6	-17.0	-17.5	-19.8	-14.1
TS2	41.7	36.2	31.8	24.7	23.9	23.9	36.7	36.1
TS3	-5.3	-12.3	-6.5	-8.6	-7.1	-11.7	-8.2	-10.4
im3 $NHCl^- \cdots HF$	-5.6	-12.6	-7.5	-9.5	-8.2	-12.0	-8.3	-10.4
P₂ $HF + NHCl^-$	11.5	5.4	11.1	8.7	9.6	5.7	8.8	6.6

^aEnergies are in kcal/mol with respect to the $F^- + NH_2Cl$ reactants, and are at 0 K and do not include ZPE. ^bThe MP2 and DFT energies were calculated using the aug-cc-pVDZ basis set and the CCSD(T) calculations were based on MP2/DZ minimum geometries.

previously investigated at various levels of theory.^{27,50–52} Most recently, Szabó and Czako characterized the stationary points of $F^- + CH_3Cl$ PES by a high level focal-point analysis (FPA) approach, considering extrapolation to the complete basis set limits, electron correlation beyond the CCSD(T) method, correlation of all the electrons and scalar relativistic effects (see Figure 1 of ref 27). Similar back- and front-side S_N2 and proton transfer pathways, as observed in the $F^- + NH_2Cl$ reaction, were found for the $F^- + CH_3Cl$ reaction. Both reactions have the double well potential model for the back-side S_N2 pathway, and the energies of all stationary points on this pathway are lower than the reactants, as shown in Figure 1. The discrepancies about the bonding type of the complexes and the barrier heights of each reaction pathway are found by comparison of $S_N2@N$ and $S_N2@C$ and they can be summarized as follows.

In contrast to the pre- and postreaction complexes **im1** and **im2**, which are characterized by a $NH \cdots X$ ($X = F$ and Cl) hydrogen bond and C_1 symmetry, the corresponding carbon species are more symmetric (C_{3v}) ion-dipole complexes $F^- \cdots CH_3Cl$ and $FCH_3 \cdots Cl^-$. Moreover, a C_s hydrogen-bonded intermediate $F^- \cdots HCH_2Cl$ was also located as a minimum in the $F^- + CH_3Cl$ entrance channel, and its transformation to the ion-dipole complex $F^- \cdots CH_3Cl$ results in only a small change of ~ 1.3 kcal/mol in the potential energy. The $F^- + CH_3Cl \rightarrow CH_3F + Cl^-$ back-side S_N2 reaction is of large reaction exothermicity and small $F^- \cdots CH_3Cl \rightarrow [F \cdots CH_3 \cdots Cl]^-$ central barrier, which are -31.9 and 3.4 kcal/mol, respectively, at the FPA level. In comparison to these results, the reaction exothermicity decreases, but the central barrier increases, for the $F^- + NH_2Cl \rightarrow NH_2F + Cl^-$ reaction, with the corresponding CCSD(T)/CBS values of -14.1 and $+18.2$ kcal/mol, respectively. The overall barriers are almost the same for both reactions with the value of -12.2 kcal/mol at FPA and CCSD(T)/CBS levels of theory, although DFT functionals yield lower overall barrier heights.

The barrier for front-side attack S_N2 pathway for $F^- + NH_2Cl$ (36.1 kcal/mol) is even higher than its C-center counterpart of 31 kcal/mol with respect to the reactants, indicating that it may play a part at higher energies. Interestingly, quasi-classical trajectory computations on an accurate global analytic $F^- + CH_3Cl$ PES have revealed a double-inversion mechanism,²⁷ in which an abstraction-induced inversion via a $FH \cdots CH_2Cl^-$ transition state is followed by a second inversion via the usual $[F \cdots CH_3 \cdots Cl]^-$ saddle point, thereby opening a substantially lower energy configuration-retaining pathway with a classical barrier height of 16.4 kcal/mol than the front-side attack mechanism. The structure of this

abstraction-induced inversion TS for the $F^- + NH_2Cl$ reaction remained elusive despite of repeated attempts to locate it. Can this double-inversion mechanism happen for the S_N2 reaction at nitrogen? The direct dynamical calculations based on current work are underway and expected to provide insights into this issue. The proton transfer reaction pathway of the $F^- + NH_2Cl$ shows a close resemblance to that of $F^- + CH_3Cl$, while the energies are considerably lowered for the former system and here only the products $HF + NHCl^-$ lie 6.6 kcal/mol higher than the reactants. As a result, the PT pathway is likely to be more competitive with the back-side S_N2 pathway in the $F^- + NH_2Cl$ reaction at low energies.

IV. CONCLUSIONS

In this work, extensive electronic structure calculations including CCSD(T), MP2, and DFT functionals M06-2X, CAM-B3LYP, B97-1, B3LYP, M06, and MPW1K have been performed to investigate the properties of stationary points on the $F^- + NH_2Cl$ PES and been compared to evaluate the accuracy of different electronic structure theories. There exist back-side and front-side S_N2 and proton transfer pathways for the $F^- + NH_2Cl$ reaction, and all pathways involve a hydrogen-bonded $F^- \cdots NH_2Cl$ complex formed by the initial association of the reactants. The double well potential model for the back-side S_N2 pathway of $F^- + CH_3Cl$ system, which is well-known for the S_N2 reactions at carbon, is also presented by its nitrogen analogue $F^- + NH_2Cl$. However, in contrast to the C_{3v} ion-dipole complexes involving carbon, the corresponding nitrogen species lose all symmetry and are characterized by a $NH \cdots X$ ($X = F$ and Cl) hydrogen bond, in line with the previous predictions.^{19,21,24} Since all the involved minima and transition states in the back-side S_N2 pathways for $F^- + NH_2Cl$ and $F^- + CH_3Cl$ systems lie below the reactants, this pathway is expected to dominate both reactions. The calculated overall barrier height for back-side S_N2 reaction at nitrogen is isoenergetic with the reaction at carbon. The front-side attack S_N2 reaction with retention of configuration is likely to be a high energy pathway for both reactions due to the involved TS lying much higher (>31 kcal/mol) than the reactants. The novel double inversion mechanism, which opens a lower energy reaction path for retention than the front-side attack for the $F^- + CH_3Cl$ reaction,²⁷ will be an interesting issue remaining to be addressed in the forthcoming $F^- + NH_2Cl$ direct dynamics calculations. When F^- reacts with NH_2Cl instead of CH_3Cl , the proton transfer pathway decrease significantly in energy and becomes more competitive with the back-side S_N2 pathway at relatively low energies.

The present studies provide useful information for understanding the $F^- + NH_2Cl$ reaction and other S_N2 reactions at nitrogen, in view of the rather limited experimental results available.^{11,17,29} It should be noted that the atomic-level dynamics may be quite different from that suggested by the stationary points and the intrinsic reaction coordinate (IRC). Hence, the detailed chemical dynamics simulations are necessary to probe the actual atomistic reaction mechanisms of the $F^- + NH_2Cl$ reaction.

The MP2 theory and DFT functionals, which are practical for direct dynamics simulations of the $F^- + NH_2Cl$ reaction, give similar representations of its PES. Their abilities to determine accurate stationary point properties for the $F^- + NH_2Cl$ PES are sensitive to the reaction pathways. Taking the predominant back-side S_N2 pathway into consideration, the best overall agreement regarding central reaction barrier and overall reactivation barriers with our *ab initio* benchmark is obtained by MP2, M06-2X, and MPW1K, with absolute errors less than 2.0 kcal/mol. These methods are recommended as the preferred ones for direct dynamics simulations. A reasonable compromise between accuracy and computational time is important for simulations. By using the aug-cc-pVDZ basis set, the M06-2X and MPW1K direct dynamics calculations are ~ 2 times faster than those with CAM-B3LYP and MP2. It will be of interest to determine whether these functionals provide an accurate representation of the dynamics at low collision energy, corresponding to the experimental temperature of 300 K,²⁹ for the $F^- + NH_2Cl$ reaction, and such dynamics simulations are ongoing.

■ ASSOCIATED CONTENT

Supporting Information

The Supporting Information is available free of charge on the ACS Publications website at DOI: 10.1021/acs.jpca.6b03487.

Stationary point geometries and frequencies calculated by MP2 and DFT functionals, potential energy curves, structural views (PDF)

■ AUTHOR INFORMATION

Corresponding Authors

*(J.Z.) E-mail: zhjx@hit.edu.cn.

*(L.Y.) E-mail: yangli2014@hit.edu.cn. Telephone: +86-451-86413708.

Notes

The authors declare no competing financial interest.

■ ACKNOWLEDGMENTS

This work is supported by the National Natural Science Foundation of China (Nos. 21573052, 21403047, 51536002), the Fundamental Research Funds for the Central Universities, China (AUGA5710012114, 5710012014), the SRF for ROCS, SEM, China, and the Open Project of Beijing National Laboratory for Molecular Sciences (no. 20140103).

■ REFERENCES

- (1) Chabinyk, M. L.; Craig, S. L.; Regan, C. K.; Brauman, J. I. Gas-phase Ionic Reactions: Dynamics and Mechanism of Nucleophilic Displacements. *Science* **1998**, *279*, 1882–1886.
- (2) Laerdahl, J. K.; Uggerud, E. Gas Phase Nucleophilic Substitution. *Int. J. Mass Spectrom.* **2002**, *214*, 277–314.

- (3) Mikosch, J.; Weidemüller, M.; Wester, R. On the Dynamics of Chemical Reactions of Negative Ions. *Int. Rev. Phys. Chem.* **2010**, *29*, 589–617.

- (4) Hase, W. L. Simulations of Gas-Phase Chemical-Reactions-Applications to S_N2 Nucleophilic-Substitution. *Science* **1994**, *266*, 998–1002.

- (5) Manikandan, P.; Zhang, J.; Hase, W. L. Chemical Dynamics Simulations of $X^- + CH_3Y \rightarrow XCH_3 + Y^-$ Gas-Phase S_N2 Nucleophilic Substitution Reactions. Nonstatistical Dynamics and Nontraditional Reaction Mechanisms. *J. Phys. Chem. A* **2012**, *116*, 3061–3080.

- (6) Yu, F. *Ab Initio* Direct Classical Trajectory Investigation on the S_N2 Reaction of F^- with NH_2F : Nonstatistical Central Barrier Recrossing Dynamics. *J. Comput. Chem.* **2012**, *33*, 401–405.

- (7) Xiong, Y.; Zhang, S. T.; Ling, X. G.; Zhang, X.; Wang, J. Y. Theoretical Investigation on Identical Anionic Halide-Exchange S_N2 Reaction Processes on N-Haloammonium Cation NH_3X^+ ($X = F, Cl, Br, \text{ and } I$). *Int. J. Quantum Chem.* **2012**, *112*, 2475–2481.

- (8) Ren, Y.; Geng, S.; Wei, X. G.; Wong, N. B.; Li, W. K. Comprehensive Theoretical Studies on the Gas Phase S_N2 Reactions of Anionic Nucleophiles toward Chloramine and N-Chlorodimethylamine with Inversion and Retention Mechanisms. *J. Phys. Chem. A* **2011**, *115*, 13965–13974.

- (9) Ulbrich, R.; Famulok, M.; Bosold, F.; Boche, G. S_N2 at Nitrogen: the Reaction of N-(4-Cyanophenyl)-O-Diphenylphosphinoylhydroxylamine with N-Methylaniline. A Model for the Reactions of Ultimate Carcinogens of Aromatic Amines with (bio) Nucleophiles. *Tetrahedron Lett.* **1990**, *31*, 1689–1692.

- (10) Helmick, J. S.; Martin, K. A.; Heinrich, J. L.; Novak, M. Mechanism of the Reaction of Carbon and Nitrogen Nucleophiles with the Model Carcinogens O-Pivaloyl-N-Arylhydroxylamines: Competing S_N2 Substitution and S_N1 Solvolysis. *J. Am. Chem. Soc.* **1991**, *113*, 3459–3466.

- (11) Anbar, M.; Yagil, G. The Hydrolysis of Chloramine in Alkaline Solution. *J. Am. Chem. Soc.* **1962**, *84*, 1790–1796.

- (12) Liu, H. Y.; Muller-Plathe, F.; van Gunsteren, W. F. Molecular Dynamics with a Quantum-Chemical Potential: Solvent Effects on an S_N2 Reaction at Nitrogen. *Chem. - Eur. J.* **1996**, *2*, 191–195.

- (13) Xing, Y. M.; Xu, X. F.; Cai, Z. S.; Zhao, X. Z. DFT Study on the Behavior and Reactivity of Electron Transfer in Gas-Phase Symmetric $X_a^- + NH_2X_b \rightarrow X_aNH_2 + X_b^-$ ($X = F, Cl, Br \text{ and } I$) Reactions. *J. Mol. Struct.: THEOCHEM* **2004**, *671*, 27–37.

- (14) Xing, Y. M.; Xu, X. F.; Cai, Z. S.; Zhao, X. Z.; Cheng, J. P. Correlation Between the Energy and Electron Density Representations of Reactivity: mPW1K Study of the Asymmetric S_N2 Reactions at the Saturated Nitrogen. *Chem. Phys.* **2004**, *298*, 125–134.

- (15) Geerke, D. P.; Thiel, S.; Thiel, W.; van Gunsteren, W. F. Combined QM/MM Molecular Dynamics Study on a Condensed-Phase S_N2 Reaction at Nitrogen: The Effect of Explicitly Including Solvent Polarization. *J. Chem. Theory Comput.* **2007**, *3*, 1499–1509.

- (16) Ren, Y.; Wei, X. G.; Ren, S. J.; Lau, K. C.; Wong, N. B.; Li, W. K. The α -Effect Exhibited in Gas-Phase $S_N2@N$ and $S_N2@C$ Reactions. *J. Comput. Chem.* **2013**, *34*, 1997–2005.

- (17) Beak, P.; Li, J. The Endocyclic Restriction Test: Experimental Evaluation of Transition-Structure Geometry for a Nucleophilic Displacement at Neutral Nitrogen. *J. Am. Chem. Soc.* **1991**, *113*, 2796–2797.

- (18) Minyaev, R. M.; Wales, D. J. Gradient Line Reaction Path for an S_N2 Reaction at Neutral Nitrogen. *J. Phys. Chem.* **1994**, *98*, 7942–7944.

- (19) Bühl, M.; Schaefer, H. F., III S_N2 Reaction at Neutral Nitrogen: Transition State Geometries and Intrinsic Barriers. *J. Am. Chem. Soc.* **1993**, *115*, 9143–9147.

- (20) Bühl, M.; Schaefer, H. F., III Theoretical Characterization of the Transition Structure for an S_N2 Reaction at Neutral Nitrogen. *J. Am. Chem. Soc.* **1993**, *115*, 364–365.

- (21) Glukhovtsev, M. N.; Pross, A.; Radom, L. Gas-Phase Identity S_N2 Reactions of Halide Ions at Neutral Nitrogen: A High-Level Computational Study. *J. Am. Chem. Soc.* **1995**, *117*, 9012–9018.

- (22) Ren, Y.; Wolk, J. L.; Hoz, S. The Performance of Density Function Theory in Describing Gas-Phase S_N2 Reactions at Saturated Nitrogen. *Int. J. Mass Spectrom.* **2002**, *221*, 59–65.
- (23) Ren, Y.; Zhu, H. J. A G2(+) Level Investigation of the Gas-Phase Non-Identity S_N2 Reactions of Halides with Halodimethylamine. *J. Am. Soc. Mass Spectrom.* **2004**, *15*, 673–680.
- (24) Yang, J.; Ren, Y.; Zhu, H. J.; Chu, S. Y. Gas-Phase Non-Identity S_N2 Reactions at Neutral Nitrogen: A Hybrid DFT Study. *Int. J. Mass Spectrom.* **2003**, *229*, 199–208.
- (25) Yu, F. Assessment of Ab Initio MP2 and Density Functionals for Characterizing the Potential Energy Profiles of the S_N2 Reactions at N Center. *J. Comput. Chem.* **2012**, *33*, 1347–1352.
- (26) Yu, F.; Song, L.; Zhou, X. G. Ab Initio Molecular Dynamics Investigations on the S_N2 Reactions of OH^- with NH_2F and NH_2Cl . *Comput. Theor. Chem.* **2011**, *977*, 86–91.
- (27) Szabó, I.; Czakó, G. Revealing a Double-Inversion Mechanism for the $F^- + CH_3Cl$ S_N2 Reaction. *Nat. Commun.* **2015**, *6*, 5972.
- (28) Stei, M.; Carrascosa, E.; Kainz, M. A.; Kelkar, A. H.; Meyer, J.; Szabó, I.; Czakó, G.; Wester, G. Influence of the Leaving Group on the Dynamics of A Gas-Phase S_N2 Reaction. *Nat. Chem.* **2016**, *8*, 151–156.
- (29) Gareyev, R.; Kato, S.; Bierbaum, V. M. Gas Phase Reactions of NH_2Cl with Anionic Nucleophiles: Nucleophilic Substitution at Neutral Nitrogen. *J. Am. Soc. Mass Spectrom.* **2001**, *12*, 139–143.
- (30) Hehre, W. J.; Radom, L.; Schleyer, P. V. R.; Pople, J. A. *Ab Initio Molecular Orbital Theory*; Wiley: New York, 1986.
- (31) Adams, G. F.; Bent, G. D.; Bartlett, R. J.; Purvis, G. D. In *Potential Energy Surfaces and Dynamics Calculations*; Truhlar, D. G., Ed.; Plenum: New York, 1981; p 133.
- (32) Zhao, Y.; Truhlar, D. G. The M06 Suite of Density Functionals for Main Group Thermochemistry, Thermochemical Kinetics, Non-covalent Interactions, Excited States, and Transition Elements: two New Functionals and Systematic Testing of Four M06-Class Functionals and 12 other Functionals. *Theor. Chem. Acc.* **2008**, *120*, 215–241.
- (33) Yanai, T.; Tew, D. P.; Handy, N. C. A New Hybrid Exchange-Correlation Functional Using the Coulomb-Attenuating Method (CAM-B3LYP). *Chem. Phys. Lett.* **2004**, *393*, 51–57.
- (34) Hamprecht, F. A.; Cohen, A. J.; Tozer, D. J.; Handy, N. C. Development and Assessment of New Exchange-Correlation Functionals. *J. Chem. Phys.* **1998**, *109*, 6264–6271.
- (35) Becke, A. D. Density-Functional Thermochemistry. III. The Role of Exact Exchange. *J. Chem. Phys.* **1993**, *98*, 5648–5652.
- (36) Dunning, H. T., Jr. Gaussian-Basis Sets for Use in Correlated Molecular Calculations 0.1. the Atoms Boron Through Neon and Hydrogen. *J. Chem. Phys.* **1989**, *90*, 1007–1023.
- (37) Woon, D. E.; Dunning, H. T., Jr. Gaussian-Basis Sets for Use in Correlated Molecular Calculations. III. the Atoms Aluminum Through Argon. *J. Chem. Phys.* **1993**, *98*, 1358–1371.
- (38) Fukui, K. The Path of Chemical Reactions-The IRC Approach. *Acc. Chem. Res.* **1981**, *14*, 363–368.
- (39) Raghavachari, K.; Trucks, G. W.; Pople, J. A.; Head-Gordon, M. A Fifth-Order Perturbation Comparison of Electron Correlation Theories. *Chem. Phys. Lett.* **1989**, *157*, 479–483.
- (40) Peterson, K. A.; Woon, D. E.; Dunning, T. H., Jr. Benchmark calculations with correlated molecular wave functions. IV. The classical barrier height of the $H+H_2 \rightarrow H_2+H$ reaction. *J. Chem. Phys.* **1994**, *100*, 7410–7415.
- (41) Valiev, M.; Bylaska, E. J.; Govind, N.; Kowalski, K.; Straatsma, T. P.; van Dam, H. J. J.; Wang, D.; Nieplocha, J.; Apra, E.; Windus, T. L.; de Jong, W. A. NWChem: A Comprehensive and Scalable Open-Source Solution for Large Scale Molecular Simulations. *Comput. Phys. Commun.* **2010**, *181*, 1477–1489.
- (42) Frisch, M. J. et al. *Gaussian 09*, Revision A.01; Gaussian, Inc.: Wallingford, CT, 2009.
- (43) Christen, D.; Minkwitz, R.; Nass, R. Microwave Spectrum, Inversion, and Molecular Structure of Monofluoramine, FNH_2 . *J. Am. Chem. Soc.* **1987**, *109*, 7020–7024.
- (44) Harmony, M. D.; Laurie, V. W.; Kuczkowski, R. L.; Schwendeman, R. H.; Ramsay, D. A.; Lovas, F. J.; Lafferty, W. J.; Maki, A. G. Molecular Structures of Gas-Phase Polyatomic Molecules Determined by Spectroscopic Methods-American Institute of Physics. *J. Phys. Chem. Ref. Data* **1979**, *8*, 619–721.
- (45) Huber, K. P.; Herzberg, G. *Molecular Spectra and Molecular structure: Constants of Diatomic Molecules*; Van Nostrand: New York, 1979.
- (46) Glukhovtsev, M. N.; Pross, A.; Radom, L. Gas-Phase Identity S_N2 Reactions of Halide Ions at Neutral Nitrogen: A High-Level Computational Study. *J. Am. Chem. Soc.* **1995**, *117*, 9012–9018.
- (47) Masuko, E.; Shin, S.; Hamada, Y. High Resolution FTIR Study on NH_2Cl Molecule: Inversion and Anharmonicity. *J. Mol. Spectrosc.* **2001**, *207*, 39–53.
- (48) Lemmon, E.; McLinden, M.; Friend, D.; Linstrom, P.; Mallard, W. *NIST Chemistry WebBook*; National Institute of Standards and Technology: Gaithersburg MD, 2011.
- (49) Müller, H.; Franke, R.; Vogtner, S.; Jaquet, R.; Kutzelnigg, W. Toward Spectroscopic Accuracy of Ab Initio Calculations of Vibrational Frequencies and Related Quantities: A Case Study of the HF Molecule. *Theor. Chem. Acc.* **1998**, *100*, 85–102.
- (50) Su, T.; Wang, H. B.; Hase, W. L. Trajectory Studies of S_N2 Nucleophilic Substitution. 7. $F^- + CH_3Cl \rightarrow FCH_3 + Cl^-$. *J. Phys. Chem. A* **1998**, *102*, 9819–9828.
- (51) Glukhovtsev, M. N.; Pross, A.; Radom, L. Gas-Phase Non-Identity S_N2 Reactions of Halide Anions with Methyl Halides: A High-Level Computational Study. *J. Am. Chem. Soc.* **1996**, *118*, 6273–6284.
- (52) Wang, H. B.; Hase, W. L. Kinetics of $F^- + CH_3Cl$ S_N2 Nucleophilic Substitution. *J. Am. Chem. Soc.* **1997**, *119*, 3093–3102.